Binuclear Metal Carbonyl R-DAB Complexes. Part XIII*. Reduction of Coordinated 1,4-diaza-1,3-butadiene to Dianionic 1,2-diaminoethane by $[HFe(CO)_4]^-$. Molecular Structure of $[(\mu\text{-H})FeMn(CO)_6\{\mu,\mu'\text{-N}(p\text{-Tol})CH_2CH_2N(p\text{-Tol})\}]$, a Pseudo-symmetrical Hetero-dinuclear Species

JAN KEIJSPER, PAUL GRIMBERG, GERARD VAN KOTEN, KEES VRIEZE**

Anorganisch Chemisch Laboratorium, University of Amsterdam, Nieuwe Achtergracht 166, 1018 WV Amsterdam, The Netherlands

MARTIN CRISTOPHERSEN and CASPER H. STAM

Laboratorium voor Kristallografie, University of Amsterdam, Nieuwe Achtergracht 166, 1018 WV Amsterdam, The Netherlands

Received October 9, 1984

Abstract

Reaction of $[MnBr(CO)_3(p\text{-Tol–DAB})]$ (*p*-Tol-DAB = (*p*-Tol)N=CH–CH=N(*p*-Tol); DAB = 1,4-diaza-1,3-butadiene) with excess $[HFe(CO)_4]^-$ and subsequent protonation yielded the heterodinuclear species $[(\mu\text{-H})FeMn(CO)_6\{\mu,\mu'\text{-N}(p\text{-Tol})CH_2CH_2N(p\text{-Tol})\}]$. During the reaction neutral, 4e-bonded *p*-Tol-DAB is reduced to formally dianionic, 8e-bonded 1,2-di-*para*-tolylaminoethane, as evidenced by an X-ray structure determination.

Crystals of $C_{22}H_{19}FeMnN_2O_6$ are monoclinic, space group $P2_1/a$ and cell constants: $a = 21.996(2)$, $b = 6.858(1)$, $c = 15.546(5)$ Å and $\beta = 110.20(1)°$; $Z = 4$. 2514 reflections have been used in the refinement resulting in a final *R*-value of 0.042.

Despite the presence of two different metal atoms in this heterodinuclear compound, the structure exhibits a nearly perfect $C_{2v}\text{-}mm_2$ symmetry with the Mn and Fe atoms being indistinguishable by crystallographic means. Each metal atom is almost ideally octahedrally surrounded by N(1), N(2) and H(30) in bridging positions and by three terminally bonded carbonyl groups.

The Mn–Fe distance of 2.5393(9) Å is the shortest Mn–Fe distance yet reported. This bond is bridged by the hydride H(30) with normal and not significantly different bond lengths of 1.83(6) and 1.70(6) Å. The metal–metal bond is also bridged by the formally dianionic, 8e-donating 1,2-di-*para*-tolylamino ethane ligand, through both nitrogen atoms with four almost equal metal nitrogen bond lengths of 2.029 Å. All 18 atoms of the C,N-backbone of this ligand are in one plane, which is perpendicular to the Fe–H(30)–Mn plane. The intraligand bond lengths and angles are consistent with a reduction of both C=N double bonds of the α-diimine.

Spectroscopic (^{1}H and ^{13}C NMR, FD mass and IR) and analytical data are consistent with a structure as found in the solid state. The bridging hydride resonates (^{1}H NMR) at rather low field: −10.02 ppm.

Reaction of $[MnBr(CO)_3(p\text{-Tol-DAB})]$ with $[DFe(CO)_4]^-$ and subsequent protonation yielded $[(\mu\text{-H})FeMn(CO)_6\{\mu,\mu'\text{N}(p\text{-Tol})C(H)(D)C(D)(H)N(p\text{-Tol})\}]$, containing the two D-atoms in a *trans* geometry as evidenced by ^{1}H NMR spectroscopy. A possible reaction mechanism is discussed.

Introduction

Part of the work of our laboratory is focussed on the activation of R-DAB, when bonded to a metal carbonyl centre (R-DAB = 1,4-disubstituted-1,4-diaza-1,3-butadiene: RN=CH–CH=NR) [2]. It was observed that strong activation of the α-diimine can be achieved by η^2-C=N coordination of one or both imine bonds [1, 2]. Until now, in isolated complexes, this type of coordination has only been observed when the R-DAB ligand is coordinated to two metal centres [1a].†. In our systematic study towards the synthesis of these poly-nuclear R-DAB complexes, two different strategies are followed.

---

*For earlier Parts see ref. [1].

**Author to whom correspondence should be addressed.

†However, after photolysis of $[Fe(CO)_3(R\text{-DAB})]$ in a matrix at 10 K, some IR-evidence has been obtained for a 4e, η^2-C=N, η^2-C'=N'-bonded R-DAB ligand; see ref. [3].

0020-1693/85/$3.30

Firstly, reaction of polynuclear carbonyls, e.g. $Ru_3(CO)_{12}$, $Fe_2(CO)_9$, $Os_3(CO)_{12}$, $Co_2(CO)_8$ with R-DAB [4].

Secondly, formation of (hetero)polynuclear complexes by doing reactions of general type: $M^- + M'$-$Br(CO)_3$(R-DAB) (M^- = $[M'(CO)_5]^-$, $[(C_5H_5)Fe(CO)_2]^-$, $[Co(CO)_4]^-$; M′ = Mn, Re) [1a, 1b, 1d, 5]. In the starting complex, [M $Br(CO)_3$(R-DAB)], the R-DAB ligand is coordinated in its normal, chelating 4e-bonding mode fashion. In all above mentioned reactions dinuclear species were indeed obtained and in some of these products the R-DAB ligand used its π-electrons for coordination [1a, 1b, 1d, 5].

Recently, we found that reaction of $[MnBr(CO)_3$(alkyl-DAB)] with $[HFe(CO)_4]^-$ yielded heterodinuclear species in which the alkyl-DAB ligand was partly reduced by the Fe-reagent and converted to a monoanionic 3-alkylamino-1-alkylazaallylic moiety (see Fig. 1) [1a].

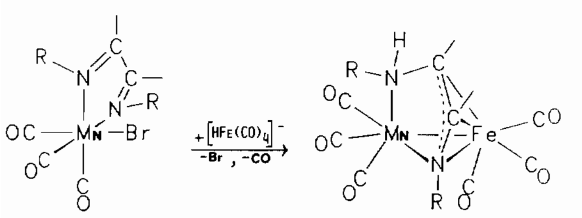

Fig. 1. Formation of $[Fe\overline{Mn(CO)_6\{RNC(H)C(H)N}(H)R\}]$ from $[HFe(CO)_4]^-$ and $[MnBr(CO)_3$(R-DAB)].

$[HFe(CO)_4]^-$ is a well known hydrogenation-, carbonylation- but especially reduction-agent, for a large variety of double and triple bonds [6]. Interestingly, in the reaction depicted in Fig. 1, the H-atom of the iron-hydride reagent ends up not at a C-atom, as may be expected for H^--migration to a C=N double bond but at the imine N-atom.

Bearing all this in mind, we were interested in studying the effect of replacing the alkyl-substituents with the *p*-Tol ones. UV spectroscopic and electrochemical measurements have shown that the LUMO of aryl-DAB's is situated at lower energy than that of alkyl-DAB's, resulting in a greater reduction ability for the former [7]. In this paper we report the results of this study, showing that the reaction of $[MnBr(CO)_3$(*p*-Tol-DAB)] with excess $[HFe(CO)_4]^-$ produces a heterodinuclear species, containing a fully reduced ligand which has two new C(ligand)–H bonds.

Experimental

Materials and Apparatus

NMR spectra were obtained on a Bruker WM250-(^1H) and on a Bruker WP80-(^{13}C) spectrometer. IR spectra were recorded with a Perkin-Elmer 283-spectrophotometer and mass spectra on a Varian-MAT 711-mass spectrometer applying field desorption (FD) technique [8]. Elemental analyses were obtained from the section Elemental Analysis of the Institute for Applied Chemistry, TNO, Utrecht, The Netherlands.

$[MnBr(CO)_3$(*p*-Tol-DAB)] and a THF solution of $Na[HFe(CO)_4]$, or $Na[DFe(CO)_4]$ have been prepared according to literature procedures [1a, 1b, 9].

Synthesis of [(μ-H)FeMn(CO)$_6$\{μ,μ′-N(p-Tol)CH$_2$CH$_2$N(p-Tol)\}]

A THF solution of $Na[HFe(CO)_4]$, obtained from 10 mmol of $Fe(CO)_5$, was added to 3 mmol of $[MnBr(CO)_3$(*p*-Tol-DAB)] and then stirred for 16 h at 40 °C and filtered. Hydrochloric acid (3 mmol of *ca.* 0.1 M) was added to the filtrate and the reaction mixture stirred for one hour. After evaporation, the residue was purified by column chromatography. Elution with first hexane and then hexane/ether (3/1) yielded a greenish fraction, identified as $Fe_3(CO)_{12}$ by IR spectroscopic means. Subsequent elution with hexane/ether (1/2) yielded a red fraction which was collected. Evaporation of the solvent and crystallization at –80 °C from ether/pentane (2/1) yielded red crystals in about 50% yield (based on Mn), identified as [(μ-H)FeMn$(CO)_6$-{μ,μ′-N(*p*-Tol)CH_2CH_2N(*p*-Tol)}] by elemental analysis, IR, ^1H NMR, ^{13}C NMR and FD-mass spectroscopy (see Tables IV and V) and an X-ray structure determination (*vide infra*). Protonation could also be carried out by stirring the filtered reaction mixture with activated silica, instead of acid. Reaction with $[DFe(CO)_4]^-$, prepared from D_2O, NaOD and $Fe(CO)_5$ in methanol-d_4 was carried out using the same procedure as discussed above.

Crystal Structure Determination of [(μ-H)FeMn(CO)$_6$\{μ,μ′-N(p-Tol)CH$_2$CH$_2$N(p-Tol)\}]

$C_{22}H_{19}FeMnN_2O_6$: hydrido(1,2-*dipara*-tolylaminoethane)hexacarbonylironmanganese.

Crystals of the title compound are monoclinic, space group $P2_1/a$, $Z = 4$. The unit cell has the dimensions: a = 21.996(2), b = 6.858(1), c = 15.546(5) Å, β = 110.20(1)°; V = 2200.9 Å^3. 4068 independent reflections ($2.5 < \theta < 65°$; $-25 < h < 24$, $0 < k < 8$, $0 < l < 18$) were measured on a NONIUS CAD4 single crystal diffractometer, using graphite monochromated CuK_α radiation. 1554 of these reflections were below the $3\sigma(I)$ level and treated as unobserved. Crystal dimensions were: 0.10 X 0.15 X 0.25 mm; d(calc.) = 1.56 g cm^{-3}; $\mu(CuK_\alpha)$ = 103.7 cm^{-1}.

The Mn and Fe positions were derived from E^2 Patterson synthesis and the rest of the non-hydrogen atoms were found in a subsequent ΔF synthesis. After isotropic block-diagonal least-squares refinement (R = 0.086), an empirical absorption correction was applied [10], after which anisotropic refinement

TABLE I. The Atomic Coordinates (e.s.d.) of $[(\mu\text{-H})\text{FeMn(CO)}_6\{\mu,\mu'\text{-N}(p\text{-Tol})\text{CH}_2\text{CH}_2\text{N}(p\text{-Tol})\}]$.

Atom	x	y	z	σx	σy	σz
Fe	0.43457	0.14009	0.28408	0.00003	0.00011	0.00005
Mn	0.31294	0.14791	0.20050	0.00003	0.00012	0.00005
N1	0.36390	0.23650	0.32990	0.00020	0.00060	0.00030
N2	0.38140	0.33720	0.19160	0.00020	0.00060	0.00030
C1	0.36540	0.45010	0.33030	0.00030	0.00080	0.00040
C2	0.37570	0.51500	0.24270	0.00030	0.00080	0.00040
C3	0.35410	0.15680	0.41040	0.00030	0.00080	0.00040
C4	0.35080	0.27240	0.48130	0.00030	0.00100	0.00040
C5	0.34080	0.18830	0.55780	0.00040	0.00100	0.00040
C6	0.33330	−0.00910	0.56460	0.00030	0.00110	0.00040
C7	0.33700	−0.12240	0.49500	0.00030	0.00090	0.00050
C8	0.34780	−0.04370	0.41850	0.00030	0.00090	0.00040
C9	0.32310	−0.09490	0.64920	0.00040	0.00140	0.00050
C10	0.39160	0.38580	0.10630	0.00030	0.00080	0.00040
C11	0.39680	0.57430	0.08000	0.00030	0.00090	0.00050
C12	0.40690	0.61420	−0.00120	0.00030	0.00080	0.00050
C13	0.41260	0.46990	−0.05850	0.00030	0.00100	0.00040
C14	0.40770	0.27530	−0.03310	0.00030	0.00110	0.00040
C15	0.39770	0.23910	0.04860	0.00030	0.00090	0.00040
C16	0.42470	0.51180	−0.14760	0.00040	0.00130	0.00050
C17	0.46700	−0.05010	0.36840	0.00030	0.00080	0.00040
C18	0.49840	0.30400	0.34570	0.00030	0.00100	0.00050
C19	0.48340	0.04580	0.22190	0.00030	0.00090	0.00040
C20	0.26410	−0.03710	0.22710	0.00030	0.00090	0.00040
C21	0.24600	0.31600	0.17430	0.00030	0.00080	0.00040
C22	0.28420	0.05930	0.08430	0.00030	0.00090	0.00040
H1 A	0.32400	0.49100	0.33400	0.00300	0.00800	0.00400
H1 B	0.39700	0.50100	0.37900	0.00300	0.00800	0.00400
H2 A	0.33900	0.58300	0.19200	0.00400	0.01100	0.00500
H2 B	0.41400	0.60200	0.25700	0.00200	0.00700	0.00300
H4	0.36000	0.39600	0.48400	0.00300	0.00800	0.00400
H5	0.33500	0.27900	0.60400	0.00300	0.01200	0.00500
H7	0.33600	−0.28800	0.49600	0.00300	0.01100	0.00400
H8	0.34700	−0.12100	0.37400	0.00200	0.00700	0.00300
H91	0.28300	−0.03200	0.68200	0.01000	0.03000	0.01400
H92	0.29300	−0.19000	0.63100	0.00300	0.01000	0.00400
H93	0.36500	−0.12800	0.70000	0.00500	0.01700	0.00900
H11	0.38700	0.68100	0.11100	0.00200	0.00800	0.00400
H12	0.40900	0.73300	−0.01800	0.00200	0.00700	0.00300
H14	0.41200	0.14700	−0.07500	0.00400	0.01300	0.00600
H15	0.39400	0.12600	0.06200	0.00300	0.00800	0.00400
H161	0.44500	0.43100	−0.16900	0.00700	0.02100	0.01000
H162	0.46500	0.61000	−0.13600	0.00400	0.01300	0.00700
H163	0.39900	0.59300	−0.18600	0.00500	0.01400	0.00700
H30	0.37000	−0.03000	0.22200	0.00300	0.00900	0.00400
O17	0.48950	−0.16950	0.42100	0.00030	0.00070	0.00040
O18	0.54050	0.40670	0.38480	0.00030	0.00080	0.00050
O19	0.51740	−0.02260	0.18740	0.00030	0.00080	0.00040
O20	0.23100	−0.15680	0.23790	0.00030	0.00070	0.00040
O21	0.20200	0.41870	0.15640	0.00020	0.00070	0.00030
O22	0.26250	−0.00040	0.01210	0.00030	0.00090	0.00030

converged to $R = 0.042$ for the 2514 observed reflections. During the final cycles the hydrogen atoms which were indicated in a ΔF-synthesis, were included isotropically in the refinement. A weighting scheme $\omega = 1/(4.36 + F_o + 0.0203F_o^2)$ was employed and the anomalous scattering of Mn and Fe was taken into account. The resulting structure exhibits a nearly perfect mirror plane, which bisects and is perpendicular to the Mn–Fe vector. Interchanging Mn and Fe had no significant effect and as a result

TABLE II. The Bond Lengths[a] (e.s.d.) in Å for $[(\mu\text{-H})FeMn(CO)_6\{\mu,\mu'\text{-N}(p\text{-Tol})CH_2CH_2N(p\text{-Tol})\}]$.

The metal carbonyl part.		The intra-ligand part	
Fe–Mn	2.5393(9)	N(1)–C(1)	1.465(7)
Fe–C(17)	1.812(6)	C(1)–C(2)	1.522(10)
Fe–C(18)	1.795(6)	C(2)–N(2)	1.484(8)
Fe–C(19)	1.795(7)	N(1)–C(3)	1.448(8)
Mn–C(20)	1.801(7)	N(2)–C(10)	1.458(9)
Mn–C(21)	1.802(6)	C(3)–C(4)	1.380(9)
Mn–C(22)	1.801(6)	C(10)–C(11)	1.373(9)
C(17)–O(17)	1.142(7)	C(4)–C(5)	1.406(10)
C(18)–O(18)	1.155(8)	C(11)–C(12)	1.383(12)
C(19)–O(19)	1.159(10)	C(5)–C(6)	1.372(10)
C(20)–O(20)	1.147(9)	C(12)–C(13)	1.366(10)
C(21)–O(21)	1.151(8)	C(6)–C(7)	1.357(10)
C(22)–O(22)	1.134(7)	C(13)–C(14)	1.406(10)
		C(7)–C(8)	1.399(11)
The metal–ligand part		C(14)–C(15)	1.384(10)
Fe–N(1)	2.031(5)	C(8)–C(3)	1.392(8)
Fe–N(2)	2.025(4)	C(15)–C(10)	1.385(9)
Mn–N(1)	2.029(4)	C(6)–C(9)	1.526(11)
Mn–N(2)	2.029(5)	C(13)–C(16)	1.525(11)
The metal–hydride part			
Mn–H(30)	1.70(6)		
Fe–H(30)	1.83(6)		

[a] Mn and Fe are crystallographic indistinguishable; the atom numbering used is that shown in Fig. 2; the C–H bond lengths are within normal range (0.81–1.24 Å).

these atoms are crystallographically indistinguishable. In the parameter list, the metal atom having the atomic coordinates: $x/a = 0.31294(3)$, $y/b = 0.14791(12)$, $z/c = 0.20050(5)$ has been arbitrarily assigned to Mn. The computer programs used for plotting [10b], the scattering factors and dispersion correction [10c], were taken from the literature*.

The molecular geometry of $[(\mu\text{-H})FeMn(CO)_6\{\mu,\mu'\text{-N}(p\text{-Tol})CH_2CH_2N(p\text{-Tol})\}]$ with the numbering of the atoms, is shown in a PLUTO-drawing [10b] of the molecule in Fig. 2. Atomic coordinates, bond lengths and selected bond angles are given in Tables I, II, III, respectively.

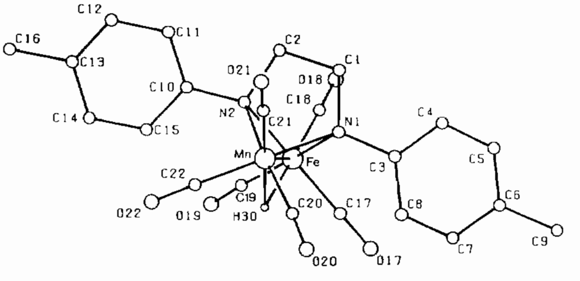

Fig. 2. Molecular geometry of $[(\mu\text{-H})FeMn(CO)_6\{\mu,\mu'\text{-N}(p\text{-Tol})CH_2CH_2N(p\text{-Tol})\}]$.

Analytical Data

Analytical data, the ν(CO) IR absorptions and the FD mass spectroscopic results are listed in Table IV.

Results

Molecular Structure

The molecular geometry together with the atomic numbering is shown in Fig. 2. Because Mn and Fe were found to be crystallographic indistinguishable as a result of the high molecular symmetry, the metal atoms are arbitrarily assigned (*vide supra*).

Atomic coordinates, bond lengths and selected bond angles are given in Tables I, II and III, respectively.

Neglecting the difference between the two metal atoms, the molecule possesses an almost ideal C_{2v}-$mm2$ symmetry with the two-fold axis through the bridging H(30)-atom, perpendicular to the Fe–Mn bond. Each metal exhibits nearly perfect octahedral coordination, being surrounded by three terminal carbonyls, two bridging nitrogen atoms and the bridging hydride H(30). The metal carbonyl part has the normal 'saw-horse' structure with an eclipsed $(CO)_3MnFe(CO)_3$ configuration. Distortions from the octahedral surroundings on both metal atoms can be derived from the bond angles deviating from 180° or 90° (see Table III). The largest deviation is the bite angle of N(1)–M–N(2) (73.0°), which is a normal value for di-N-bridged dinuclear species [11]. In other species of this type, containing two N-atoms symmetrically linking two $M(CO)_3$-units (M = Fe, Co), a bent metal–metal bond has been suggested in order to preserve the octahedral geometry of both metals**. The symmetrically bridging hydride atom in the compound (Fe–H(30) = 1.83(6) being at the 3σ-level equivalent to Mn–H(30) = 1.70(6) Å) has a position that would correspond with the midpoint of such a bent bond. Thus the intersection angle of the (with respect to H(30)) *trans* OC–M vectors, being 98°, fits nicely with the observed Mn–H(30)–Fe-angle of 91.8(29)°, which is a relatively small 'hydride' angle [13]. It has been often noted that a bridging hydride is usually located 'inside' the intersection of the *trans* ligand–metal vectors [12].

Normally, a bridging hydride has a lengthening effect on a metal–metal separation [see *e.g.* [12c]]. The Mn–Fe bond length in the present compound (2.5393(9) Å), however, is the shortest one yet reported. In other dinuclear MnFe-complexes the metal–metal bond lengths vary between 2.84 and

---

*Tables of observed and calculated structure factors, the final anisotropic thermal parameters, and all bond lengths and angles are available on request from the author.

**See *e.g.* ref. [11] and ref. [15].

TABLE III. Selected Bond Angles[a] (e.s.d.) in ° within [(μ-H)FeMn(CO)$_6${μ,μ'-N(*p*-Tol)CH$_2$CH$_2$N(*p*-Tol)}].

The metal carbonyl part					
Fe–C(17)–O(17)	177.5(7)	Fe–C(19)–O(19)	175.0(5)	Mn–C(21)–O(21)	177.9(5)
Fe–C(18)–O(18)	178.4(7)	Mn–C(20)–O(20)	175.4(5)	Mn–C(22)–O(22)	175.5(7)
Around Fe				Around Mn	
Mn–Fe–N(1)	51.2(1)			Fe–Mn–N(1)	51.3(1)
Mn–Fe–N(2)	51.3(1)			Fe–Mn–N(2)	51.1(1)
Mn–Fe–C(17)	117.9(2)			Fe–Mn–C(20)	118.3(2)
Mn–Fe–C(18)	138.7(2)			Fe–Mn–C(21)	139.8(2)
Mn–Fe–C(19)	116.9(2)			Fe–Mn–C(22)	116.7(2)
Mn–Fe–H(30)	41.9(20)			Fe–Mn–H(30)	46.2(20)
N(1)–Fe–N(2)	73.0(2)			N(1)–Mn–N(2)	73.0(2)
N(1)–Fe–C(17)	98.0(3)			N(1)–Mn–C(20)	98.8(2)
N(1)–Fe–C(18)	99.3(3)			N(1)–Mn–C(21)	99.3(2)
N(1)–Fe–C(19)	168.1(2)			N(1)–Mn–C(22)	168.0(3)
N(1)–Fe–H(30)	81.0(23)			N(1)–Mn–H(30)	84.4(19)
N(2)–Fe–C(17)	168.7(3)			N(2)–Mn–C(20)	169.2(2)
N(2)–Fe–C(18)	96.6(2)			N(2)–Mn–C(21)	98.2(2)
N(2)–Fe–C(19)	99.5(2)			N(2)–Mn–C(22)	99.2(3)
N(2)–Fe–H(30)	84.2(18)			N(2)–Mn–H(30)	87.6(23)
C(17)–Fe–C(18)	91.4(3)			C(20)–Mn–C(21)	89.8(3)
C(17)–Fe–C(19)	88.3(3)			C(20)–Mn–C(22)	87.8(3)
C(17)–Fe–H(30)	87.9(18)			C(20)–Mn–H(30)	84.7(23)
C(18)–Fe–C(19)	90.6(3)			C(21)–Mn–C(22)	90.7(3)
C(18)–Fe–H(30)	179.3(18)			C(21)–Mn–H(30)	173.8(21)
C(19)–Fe–H(30)	89.2(23)			C(22)–Mn–H(30)	86.2(20)
The ligand part					
Fe–N(1)–C(1)	107.9(4)	Mn–N(1)–C(1)	107.9(3)	Mn–N(1)–Fe	77.4(2)
Fe–N(1)–C(3)	122.7(3)	Mn–N(1)–C(3)	123.2(3)	Mn–N(2)–Fe	77.6(2)
Fe–N(2)–C(2)	107.7(3)	Mn–N(2)–C(2)	106.7(4)	N(1)–C(1)–C(2)	107.4(5)
Fe–N(2)–C(10)	124.5(4)	Mn–N(2)–C(10)	124.0(3)	N(2)–C(2)–C(1)	107.7(4)
				C(1)–N(1)–C(3)	112.6(5)
				C(2)–N(2)–C(10)	111.5(4)
The hydric angle				The *p*-Tol parts	
Fe–H(30)–Mn	91.8(29)			C–C–C	120.3(20) (mean)[b]

[a] Mn and Fe are crystallographic indistinguishable; the atom numbering is the same as that shown in Fig. 2. [b] The standard deviation of the mean value is calculated by $(\Sigma_i(x_i - \bar{x})^2/N)^{1/2}$.

2.56 Å [1a,b]. In [(μ-H)FeMn(CO)$_6${C$_5$H$_4$N-2-CH=N(t-Bu)}] for example, also containing a bridging ligand and a bridging hydride, the Fe–Mn bond length is 2.7465(3) Å [1b]. It appears that the bond lengthening effect of the hydride is in the present compound more than counter-balanced by the shortening effect of the dinitrogen-ligand on this Mn–Fe distance. In other di-N-bridged dimers, very short M–M bonds are also found (M = Fe, Co; M–M ~ 2.40 Å) [11, 14]. It has been put forward that the fixed metal–ligand geometry in these types of complexes, with M–N–M-angles of about 75° and relatively short M–N bond lengths of about 2.00 Å, is the main reason for the short M–M bond lengths [11].

All eighteen atoms of the skeleton of the (*p*-Tol)NCH$_2$CH$_2$N(*p*-Tol)-ligand are in one plane (see Fig. 3; maximum deviation from the least-squares plane: 0.07 Å). This plane is perpendicular (89.98°) to the Fe–H(30)–Mn-plane.

It is not evident why the ligand system exhibits such a good planarity. On the one hand it points to a mesomeric stabilization, involving the aryl-π-system, filled p-orbitals of the right symmetry on both N-atoms and the empty [15] orbitals of a_2- or b_2-symmetry on the bimetallic unit. On the

TABLE IV. Analytical Data of $[(\mu\text{-H})FeMn(CO)_6\{\mu,\mu'\text{-N}(p\text{-Tol})CH_2CH_2N(p\text{-Tol})\}]$.

M[a] (calculated)	ν(CO)[b]	Elemental Analysis[c]	
	2080(m), 2022(m)	C	50.90 (50.99)
518 (518.2)	2014(s), 1929(s)	H	3.71 (3.70)
	1923(s)	N	5.37 (5.41)

[a]The observed M-value is for the most intense peak of the isotope pattern; the calculated M-value is based upon ^{56}Fe. [b]IR ν(CO)-absorptions recorded in hexane in which the complex is only slightly soluble; peak positions in dichloromethane: 2082(m), 2020(sh), 2008(s), 1917 (broad, m). [c]Found (calculated) %.

TABLE V. NMR Data[a] of $[(\mu\text{-H})FeMn(CO)_6\{\mu,\mu'\text{-N}(p\text{-Tol})CH_2CH_2N(p\text{-Tol})\}]$.

(^{1}H NMR):	−10.02(s, 1H) (μ-H); 3.50(d[b], 2H), 3.42(d[b], 2H) (ethane); 7.03(d[c], 4H), 7.23(d[c], 4H) (Phenyl); 2.25(s, 6H) (methyl); recorded in $CDCl_3$
(^{13}C NMR):	203.4[e] (CO); 157.6, 134.5, 127.3, 124.9 (Phenyl) 66.5 (ethane); 20.5 (methyl); recorded in toluene-d_8

[a]The values in ppm, relative to TMS (multiplicity, integral) (assignment), have been obtained at 35 °C; s = singlet, d = doublet. [b]The AA'BB' spin system of the ethane-fragment appears as a deceptively simple, broadened AB-pattern (J = 8 Hz). [c]J = 8 Hz. [e]Three more less intense peaks appear at −40 °C: 219.6, 218.8 and 220.1 ppm.

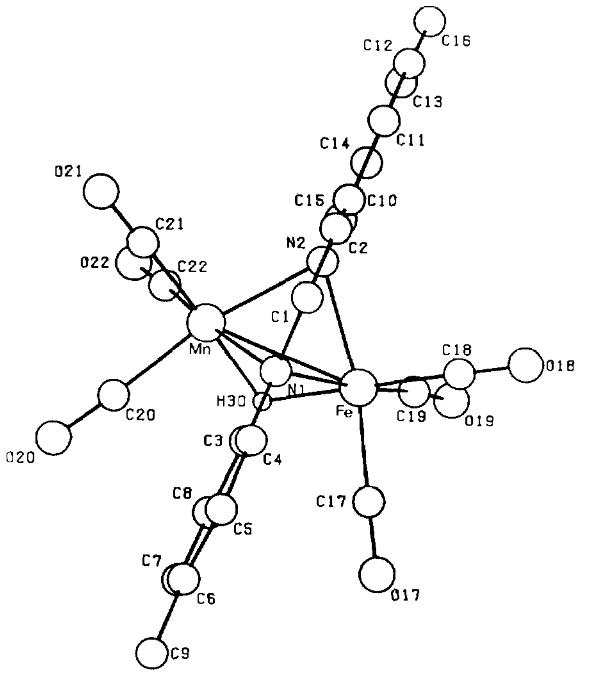

Fig. 3. View of the molecule, showing its planar ligand system.

other hand, several observations are not in line with extensive mesomeric stabilization:

(i) The N–C(aryl) bond lengths of 1.46 Å are hardly shortened with respect to normal N–C single bond lengths (1.48 Å).

(ii) In $[(PhN)_2C(O)Fe_2(CO)_6]$ [16] and in $[\{N(C_6H_4\text{-2-NPh})\}Fe_2(CO)_6]$ [16], in which species mesomeric stabilization may be expected likewise, the aryl rings are twisted about 90° out of the ligand's plane.

(iii) In solution, the aryl rings are freely rotating as evidenced by NMR spectroscopy (*vide infra*).

The N(1)–C(1)–, N(2)–C(2)– and C(1)–C(2)– intraligand bond lengths of 1.465(7), 1.484(8) and 1.522(10) Å, respectively, are consistent with a reduction of both imine-double bonds to single bonds. Also the bond angles around C(1) and C(2) (see Table III; C–C–H = 113° (mean); N–C–H = 108° (mean)) are indicative for this.

FD-mass Spectroscopy

The heteronuclear character of the complex is clearly demonstrated by its mass and isotope pattern found in the FD mass spectrum (*cf.* [1a, 1b, 8]; natural abundance of metal isotopes: ^{56}Fe, 91.7%; ^{54}Fe, 5.8%; ^{57}Fe, 2.2%; ^{55}Mn, 100%).

Only the molecular ion is observed at a m/z-value which corresponds to the overall formula $C_{22}H_{19}FeMnN_2O_6$.

IR Spectroscopy

The IR data (ν(CO) region) are collected in Table IV. Neglecting the difference between the two metals, the complex exhibits an almost perfect C_{2v}-$mm2$ symmetry in the solid state (*vide supra*). The observation of five singly degenerate IR active CO stretching frequencies in solution is in line with a retention of this symmetry. The two A_1, two B_1 and B_2 vibrations are all found in the terminal region.

^{1}H NMR Spectroscopy

The ^{1}H NMR data are listed in Table V.

Besides the molecular mass and isotope pattern observed in the FD mass spectrum, the heterodinuclear character of the complex can be derived from it's ^{1}H NMR spectrum. In a molecule of perfect C_{2v}-symmetry, the ethane-protons should give rise to one singlet only. The observation of an *AB*-pattern (J = 8 HZ) at the expected chemical shifts of *ca.* 3.5 ppm, proves that the two M(CO)$_3$-parts of the molecule are not magnetically equivalent. In theory, the protons in the fixed NCH$_2$CH$_2$N-part should appear as an AA'-BB'-type of spectrum, but a deceptively simple broadened AB-pattern is observed (see Fig. 4).

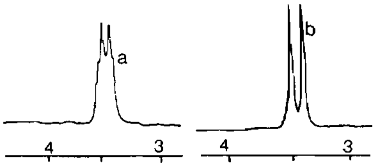

Fig. 4. ^{1}H NMR pattern for the ethane-protons of: (a) the non-deuterated complex; (b) the deuterated complex.

The two *p*-Tol groupings are equivalent and freely rotating as evidenced by the one *p*-Tol pattern observed in solution.

The bridging hydride resonates at −10.02 ppm which is at rather low field for a bridging hydride [17].

When [MnBr(CO)$_3$(*p*-Tol-DAB)] is reacted with an excess of [DFe(CO)$_4$]$^-$ followed by protonation, [(μ-H)FeMn(CO)$_6${μ,μ'-N(*p*-Tol)C(H)(D)C(D)(H)N(*p*-Tol)}] is obtained. This is proved by its ^{1}H NMR spectrum (see Fig. 4). The bridging hydride still absorbs at −10.02 ppm with an integral of one proton. The central ethane-part of the ligand, however, is changed markedly with respect to the nondeuterated complex. The protons in this part appear as two broadened singlets at 3.50 and 3.42 ppm with a total integral of two protons. These results prove that each of the two C sites contain one H and one D atom, while the integral strongly suggests the presence of one stereoisomer only (*trans*), in which case the addition-reaction is stereo-selective. The presence of a mixture of all three possible stereoisomers, however, can not be totally excluded. Some of the broadening of the signals may be due to unresolved H–D coupling and some to ^3J(H,H).

^{13}C NMR Spectroscopy (see Table V)

The general feature of the ^{13}C NMR spectrum is in line with a structure in solution being the same as that in the solid state. The reduction of the *p*-Tol-DAB ligand to the formally dianionic di-*para*-tolylamino-ethane ligand is apparent from the chemical shift of both ethane carbons of 66.5 ppm. The imine C atoms in R-DAB complexes resonate at about 180 ppm when the ligand is 4e; σ-N, σ-N'-bonded, and at about 100 ppm when the ligand is 8e; σ-N, σ-N', η^2-C=N, η^2-C'=N'-coordinated [1, 18]. The symmetry of the present compound is also reflected in the single pattern found for the two freely rotating *p*-Tol groupings.

The signal at 203.4 ppm is assigned to the three rapidly exchanging carbonyl atoms on Fe. At 233 K, this signal remains sharp and three more, hardly detectable signals, which we assign to the three carbonyls bonded to Mn, appear at: 219.6, 219.8 and 220.1 ppm.

Discussion

Reaction sequence

Although the precise reaction sequence resulting in the formation of [(μ-H)FeMn(CO)$_6${μ,μ'-N(*p*-Tol)CH$_2$CH$_2$N(*p*-Tol)}] is uncertain, a tentative scheme is given in Fig. 5.

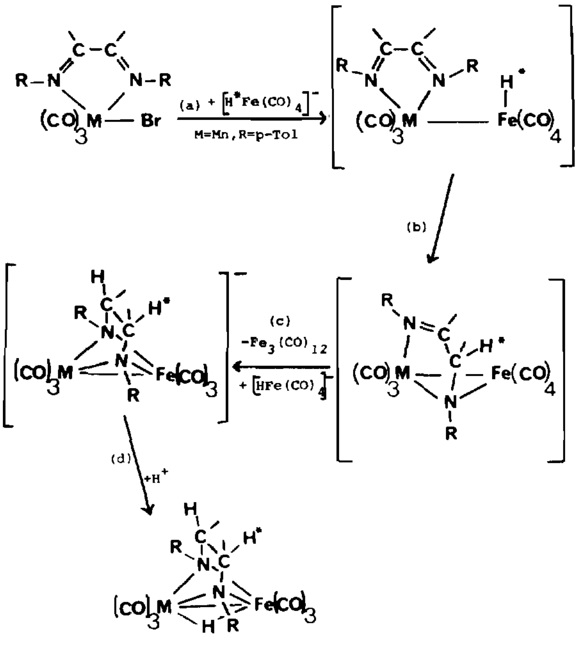

Fig. 5. A tentative reaction sequence for the formation of [(μ-H)FeMn(CO)$_6${μ,μ'-N(*p*-Tol)CH$_2$CH$_2$ N(*p*-Tol)}].

This reaction mechanism is consistent with the following three observations:

(i) Only use of an excess of [HFe(CO)$_4$]$^-$ gives reasonable yields.

(ii) Final protonation is necessary; in the reaction mixture before protonation no ν(CO) stretching frequencies due to the product are observed in the IR-spectrum.

(iii) Reaction of [MnBr(CO)$_3$(*p*-Tol-DAB)] with [DFe(CO)$_4$]$^-$ and subsequent protonation results in a product in which both ethane-carbons each bear one D-atom, presumably in a *trans*-geometry, and in which the bridging atom is a hydride.

In the first step (a), Br$^-$ is substituted for the Fe–hydride anion. This is indicated by the fact that only a heterodinuclear species can be isolated. If the reaction would proceed via an 'open' electron transfer mechanism, homodinuclear species should also be obtained [1d, 19].

In the second step (b), the precise mechanism of which is not known, an insertion of one C=N double bond into the Fe–H bond occurs, resulting in C–H bond formation. This step, which may also be described as an addition of a Fe–H moiety to an imine bond probably takes place with a '*cis*'-stereospecificity because that is often found for reactions of metal–hydrides with unsaturated systems [20]. The result is thus a *cis*-α-metallation of the N=C double bond [21].

One mechanism for step (b) involves a hydride (H$^-$)-transfer from iron to the ligand. Another possibility is a prior single-electron-transfer resulting in a [Mn(*p*-Tol-DAB)]$^{\bullet}$-radical part and a H$^{\bullet}$-radical. After H$^{\bullet}$-migration, a C–H bond is likely to be formed because the spin density in the [Mn(*p*-Tol-DAB)]$^{\bullet}$ radical part is expected to be highest on the imine-C-atoms [1a, 22, 23]. Spin density on the imine-N-atoms will be reduced as a result of delocalization over the aryl rings of the *p*-Tol substituents. A third possibility is that the addition step (b) occurs via a concerted mechanism [20]. This second reaction step, giving either N–H (R = alkyl)- or C–H (R = *p*-Tol)bond formation, may bear some resemblance with reactions of organo–Zn and –Al compounds or Grignard reagents with 1,4-(di)-hetero-1,3-butadienes (hetero-atom = N,O). These types of reactions may yield both C- and N-alkylation products [24].

In the third step (c), a second [HFe(CO)$_4$]$^-$ species reduces the remaining C=N double bond. Because of the strong polarization in this bond, the hydride will add on the imine-C-atom. Reduction of imines and other unsaturated systems by [HFe(CO)$_4$]$^-$ has been described earlier [1a, 25]. Because of steric interaction with the already coordinated Fe(CO)$_4$-unit, the reducing [HFe(CO)$_4$]$^-$ agent will approach the imine bond from opposite side. Therefore the second, new C–H bond will be in a *trans* position with respect to the first one. The resulting negative charge on the ligand is stabilized by coordination of the N-atom to Fe with concomitant loss of CO. The iron carbonyl fragments of the reducing agent probably combine to give Fe$_3$(CO)$_{12}$, which indeed has been found in the reaction mixture.

In the fourth step (d) the negative charge on the complex is neutralized by protonation with dilute acid or silica.

Comparison of Reactions of [HFe(CO)$_4$]$^-$ with [MBr(CO)$_3$(R-DAB)] (M = Mn, Re; R = alkyl, p-Tol)

Three different types of products are obtained from the reaction of [HFe(CO)$_4$]$^-$ with [MBr(CO)$_3$(R-DAB)], depending on both the nature of M and R (see Fig. 6).

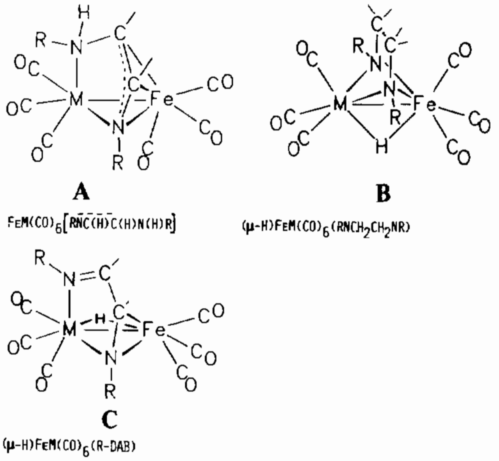

A
FeM(CO)$_6$[$\overline{\text{RNC(H)C(H)N(H)R}}$]

B
(μ-H)FeM(CO)$_6$(RNCH$_2$CH$_2$NR)

C
(μ-H)FeM(CO)$_6$(R-DAB)

Fig. 6. The three different types of products from the reaction of [HFe(CO)$_4$]$^-$ with [MBr(CO)$_3$(R-DAB)].

When M = Mn, R = alkyl [1a], product **A**; *i.e.* [Fe$\overline{\text{Mn(CO)}_6\text{\{RNC(H)C(H)N}}$(H)R\}], is the only observed product. The possible reaction routes, leading to the N–H bond formation have been discussed elswehere [1a].

When M = Mn, R = *p*-Tol [this report] and using excess [HFe(CO)$_4$]$^-$, and protonation, product **B**; *i.e.* [(μ-H)FeMn(CO)$_6$\{μ,μ'-N(*p*-Tol)CH$_2$CH$_2$N(*p*-Tol)\}], is the main product, containing two new C–H bonds. However, traces of the other two types of products (**A** and **C**) also have been obtained in yields of less than 5%. The observation that the hydride hydrogen ends up on the imine-C-atom and not, as in the case of the alkyl-DAB derivatives on the imine-N-atom (product **A**), proves that the introduction of the *p*-Tol substituents has an important electronic influence on the ligand system. The difference of N–H (product **A**) *vs.* C–H (product **B**)-bond formation may be explained by a reaction mechanism, involving a single-electron transfer (*vide supra*) [1a].

When M = Re, R = alkyl [1b], primarily [(μ-H)-FeRe(CO)$_6$(R-DAB)] is obtained, containing an unconverted α-diimine ligand. This product of type **C** is isoelectronic with the type **A** product and is probably formed via a type **A** intermediate [1a,b]. The reaction of $[HFe(CO)_4]^-$ with the α-diimine derivatives $[MBr(CO)_3(C_5H_4N\text{-}2\text{-}CH{=}NR)]$ (M = Mn, Re) is analogous and the crystal structure has been established for R = t-Bu; M = Mn [1b].

Conclusions

Neutral, coordinated *p*-Tol-DAB may be converted to the formally dianionic 1,2-di-*para*-tolylaminoethane moiety by interaction with two equivalents of $[HFe(CO)_4]^-$.

Different types of products are obtained in the reaction of [MBr(CO)$_3$(R-DAB)] (M = Mn, Re) with $[HFe(CO)_4]^-$,. depending on both M and R. Only for R = *p*-Tol, C–H bond formation is observed, proving that replacing alkyl for *p*-Tol substituents has a major electronic influence on the ligand system.

Acknowledgements

We thank Mr. Heijdenrijk for collecting the X-ray data. We also thank the Netherlands Foundation for Chemical Research (SON) and the Netherlands Organization for Pure Research (ZWO) for their financial support.

References

1 (a) J. Keijsper, J. Mul, G. van Koten, K. Vrieze, H. J. C. Ubbels and C. H. Stam, *Organometallics, 3,* 1732 (1984);
(b) J. Keijsper, P. Grimberg, G. van Koten, K. Vrieze, B. Kodic-Prodic and A. L. Spek, *Organometallics,* in press;
(c) L. H. Staal, L. H. Polm, R. W. Balk, G. van Koten, K. Vrieze and A. M. F. Brouwers, *Inorg. Chem., 19,* 3343 (1980);
(d) L. H. Staal, J. Keijsper, G. van Koten, K. Vrieze, J. A. Cras and W. P. Bosman, *Inorg. Chem., 20,* 555 (1981);
(e) J. Keijsper, L. H. Polm, G. van Koten, K. Vrieze, G. Abbel and C. H. Stam, *Inorg. Chem., 23,* 2142 (1984);
(f) L. H. Staal, G. van Koten, K. Vrieze, F. Ploeger and C. H. Stam, *Inorg. Chem., 20,* 1830 (1981).

2 (a) G. van Koten and K. Vrieze, *Adv. Organomet. Chem., 21,* 151 (1982);
(b) G. van Koten and K. Vrieze, *Recl. Trav. Chim. Pays-Bas, 100,* 129 (1981).

3 M. W. Kokkes, D. J. Stufkens and A. Oskam, *J. Chem. Soc., Chem. Commun.,* 369 (1983); *J. Chem. Soc., Dalton Trans.,* (1984) in press.

4 (a) L. H. Staal, P. Bosma and K. Vrieze, *Inorg. Chim. Acta, 43,* 125 (1980);
(b) L. H. Staal, L. H. Polm, K. Vrieze, F. Ploeger and C. H. Stam, *Inorg. Chem., 20,* 3590 (1981);
(c) L. H. Staal, L. H. Polm and K. Vrieze, *Inorg. Chim. Acta, 40,* 165 (1980);
(d) L. H. Staal, G. van Koten and K. Vrieze, *J. Organomet. Chem., 206,* 99 (1981).

5 L. H. Staal, G. van Koten and K. Vrieze, *J. Organomet. Chem., 175,* 73 (1979).

6 (a) T. Mitsudo, Y. Watanabe, H. Nakanishi, I. Morishima, T. Imibushi and Y. Takegami, *J. Chem. Soc., Dalton Trans.* 1298 (1978) and refs. therein;
(b) M. Yamashita, K. Miyoshi, Y. Okada and R. Suemitsu, *Bull. Chem. Soc. Jpn., 55,* 1329 (1982) and refs. therein.

7 H. tom Dieck and I. W. Renk, *Chem. Ber., 104,* 110 (1971).

8 L. H. Staal, G. van Koten, R. H. Fokkens and N. M. M. Nibbering, *Inorg. Chim. Acta, 50,* 205 (1981).

9 M. Y. Darensbourg, D. J. Darensbourg and H. L. C. Baros, *Inorg. Chem., 17,* 297 (1978).

10 (a) N. Walker and D. Stuart, *Acta Crystallogr., Sect. A:, 39,* 158 (1983).
(b) S. Motherwell and B. Clegg, 'PLUTO', Program for plotting Molecular and Crystal structures, Univ. of Cambrdige, Cambridge, 1978;
(c) 'International Tables for Crystallography, Vol. IV', Kynoch Press, Birmingham, 1974.

11 L. F. Dahl, W. R. Costello and R. B. King, *J. Am. Chem. Soc., 90,* 5422 (1968).

12 (a) C. Y. Wei, M. W. Marks, R. Bau, S. W. Kirtley, D. E. Bisson, M. E. Hendersson and T. F. Koetzle, *Inorg. Chem., 21,* 2556 (1982);
(b) M. A. Andrews, G. van Buskirk, C. B. Knobler and H. D. Kaesz, *J. Am. Chem. Soc., 101,* 7245 (1979);
(c) M. R. Churchill, B. G. de Boer and F. J. Rotella, *Inorg. Chem., 15,* 1843 (1976);
(d) R. Bau, R. G. Teller, S. W. Kirtley and T. F. Koetzle, *Acc. Chem. Res., 12,* 176 (1979).

13 R. G. Teller and R. Bau, *Struct. Bonding (Berlin), 41,* 1 (1981).

14 (a) R. J. Doedens, *Inorg. Chem., 7,* 2323 (1968);
(b) J. Doherty, A. R. Manning and F. S. Stephens, *Inorg. Chem., 21,* 3332 (1982);
(c) S. Otsuka, A. Nakamura and T. Yoshida, *Inorg. Chem., 7,* 261 (1968);
(d) A. de Cian, R. Weiss, Y. Chauvin, D. Commereuc and D. Hugo, *J. Chem. Soc., Chem. Commun.,* 249 (1976).

15 D. L. Thorn and R. Hoffmann, *Inorg. Chem., 17,* 126 (1978).

16 (a) J. Piron, P. Piret and M. van Meerssche, *Bull. Soc. Chim. Belg., 76,* 505 (1967);
(b) P. E. Baikie and O. S. Mills, *Inorg. Chim. Acta, 1,* 55 (1967).

17 A. P. Humphries and H. D. Kaesz, *Prog. Inorg. Chem., 25,* 146 (1979).

18 L. H. Staal, J. Keijsper, L. H. Polm and K. Vrieze, *J. Organomet. Chem., 204,* 101 (1981).

19 R. E. Dessy and P. M. Weissman, *J. Am. Chem. Soc, 88,* 5124 (1966).

20 G. Henric-Olivé and S. Olivé, *Top. Curr. Chem., 67,* 107 (1976);
R. F. Heck, in P. M. Maitlis *et al.* (eds.), 'Organotransition-Metal Chemistry, a Mechanistic Approach', Academic Press, New York, 1974.

21 A. Nakamura and S. Otsuka, *J. Mol. Catal., 1,* 285 (1975/76).

22 M. W. Kokkes, D. J. Stufkens and A. Oskam, to be published.

23 G. van Koten, J. T. B. H. Jastrzebski and K. Vrieze, *J. Organomet. Chem., 250,* 49 (1983).

24 C. Kashima, Y. Aoki and I. Omote, *J. Chem. Soc., Perkin Trans. I:,* 2511 (1975).

25 T. Mitsudo, Y. Watanabe, H. Nakanishi, J. Morishima, T. Inubushi and Y. Takegami, *J. Chem. Soc., Dalton Trans.,* 1298 (1978) and refs. therein.